Elastic and chemical contributions to the stability of magnetic surface alloys on Ru(0001)

Madhura Marathe, Mighfar Imam, and Shobhana Narasimhan
Theoretical Sciences Unit, Jawaharlal Nehru Centre for Advanced Scientific Research, Jakkur, Bangalore-560064, India
(Received 16 September 2008; revised manuscript received 2 January 2009; published 11 February 2009)

We have used density-functional theory to study the miscibility and magnetic properties of surface alloys. Our systems consist of a single pseudomorphic layer of M_xN_{1-x} on the Ru(0001) surface, where M=Fe or Co, and N=Pt, Au, Ag, Cd, or Pb. Several of the combinations studied by us display a preference for atomically mixed configurations over phase-segregated forms. We have also performed further *ab initio* calculations to obtain the parameters describing the elastic interactions between atoms in the alloy layer, including the effective atomic sizes at the surface. We find that while elastic interactions favor alloying for all the systems considered by us, in some cases chemical interactions disfavor atomic mixing. We show that a simple criterion (analogous to the Hume-Rothery first law for bulk alloys) need not necessarily work for strain-stabilized surface alloys because of the presence of additional elastic contributions to the alloy heat of formation that will tend to oppose phase segregation. We find that magnetic moments are significantly enhanced with respect to the bulk elements.

DOI: 10.1103/PhysRevB.79.085413 PACS number(s): 68.35.Dv, 68.55.−a

I. INTRODUCTION

It has been known since ancient times that alloying two metals can give rise to a new material with properties that are improved over those of the constituent metals. For example, alloys can have superior mechanical or magnetic properties, an increased resistance to corrosion, or constitute good catalysts. However, not all pairs of metals form stable alloy phases. The rules governing alloy formation in the bulk were first formulated by Hume-Rothery.[1] The first of these empirical laws states that if the atomic-size mismatch is greater than 15%, phase segregation is favored over the formation of solid solutions. Thus, many pairs of metals are immiscible (or nearly so) in the bulk.

In recent years, it has become apparent that surface science can extend the chemical phase space available for the search for new alloy systems. It has long been known that bulk alloys exhibit surface segregation so that the chemical composition at the surface can differ considerably from that in the bulk. However, the field of surface alloying gained additional interest when it was discovered that even metals that are immiscible in the bulk can form stable surface alloys as a result of the altered atomic environment at the surface.[2–4] These alloys display atomic mixing that is confined to the surface layer or, in some cases, the top few layers. These results were explained by Tersoff,[5] who argued that in cases where there is a large size mismatch, as a result of which the energetics are dominated by strain effects, alloying will be disfavored in the bulk but favored at the surface.

Subsequently, another class of surface alloys has emerged, where two metals that differ in size are co-deposited on a third metal of intermediate size. In such systems, any single-component pseudomorphic layer will be under tensile or compressive stress (that may or may not be relieved by the formation of dislocations);[6] however if the two elements were to mix, the stress would presumably be considerably relieved. Thus, the strain imposed by the presence of the substrate promotes alloying in the surface layer. Some examples of such strain-stabilized surface alloys are an Ag-Cu monolayer on Ru(0001),[7–9] Pd-Au/Ru(0001),[10] and Pb-Sn/Rh(111).[11]

Hitherto, the guiding principle in the search for such systems has been the rule of thumb that the (bulk) nearest-neighbor (NN) distance of the substrate should be the average of the NN distances of the two overlayer elements. However, this simple criterion does not necessarily work. For example, Thayer *et al.*[12,13] have studied the Co-Ag/Ru(0001) system. At first sight, this system would seem to be a good candidate for the formation of a strain-stabilized surface alloy since the NN distance for Ag is larger than that of Ru by 8%, while that of Co is smaller by 7%. However, instead of forming an atomically mixed structure, it was found that the stable structure consisted of Ag droplets surrounded by Co. After doing a combined experimental and theoretical study, these authors concluded that chemical bonding between Ag and Co is disfavored in this system, and the observed structure results from a lowering of stress at the boundary between Co and Ag islands.

In this paper, we examine ten different bimetallic systems on a Ru(0001) substrate. Some of the questions that we hope to address include: (i) is it only the mean size of the overlayer atoms that matters, or do individual sizes also matter? (ii) can one develop a criterion based on atomic size that will predict whether or not a surface alloy will form? (iii) how different are atomic sizes at the surface compared to those in the bulk? (iv) what is the relative importance of elastic and chemical interactions? (v) what role does magnetism play?

The bimetallic systems we have considered all consist of one magnetic metal M (Fe or Co) and one nonmagnetic metal N (Pt, Ag, Au, Cd, or Pb), co-deposited on Ru(0001) to form a surface alloy of the form M_xN_{1-x}/S, where S denotes the Ru substrate. Such systems, involving one magnetic and one nonmagnetic element, are of interest because alloying can, in some cases, improve magnetic properties. Conversely, in some applications,[14,15] one would prefer that instead of mixing at the atomic level, the system should spontaneously organize into a pattern consisting of alternating domains of the magnetic and the nonmagnetic element.

TABLE I. Values in Å of $(a_M+a_N)/2$, the average of the nearest-neighbor (NN) spacings of M and N in their bulk structures. By comparing these numbers with a_S, the NN distance of Ru in the bulk=2.70 Å, one expects Co-Au and Co-Ag to form stable alloys, and Pb alloys to be unstable. In this table, all the values used are experimental values, taken from Ref. 21.

	Pt	Au	Ag	Cd	Pb
Fe	2.63	2.69	2.69	2.73	2.99
Co	2.64	2.70	2.70	2.75	3.01

Ru(0001) was chosen as the substrate, in part because of its intermediate NN distance, and in part because its hardness and immiscibility with the other elements make it less likely that the alloy elements will penetrate into the bulk. The bulk NN distances, a_M, of the two magnetic metals Fe and Co, are about 7%–8% less than a_S, the NN separation in the Ru substrate, while all five nonmagnetic metals we have considered have bulk NN distances, a_N, larger than that of Ru. However, the N metals we have chosen display a large variation in size: the NN distance in Pt is approximately 3% more than that in Ru, while in Pb the discrepancy is 26%. Accordingly, only Fe-Pt and Co-Pt fall within the 15% range of the Hume-Rothery criterion for bulk alloys; alloys of Fe and Co with Au and Ag fall slightly outside this range, while those with Cd and Pb fall well outside the range. If there is a size-dependent trend that determines whether or not alloying is favored, then one might hope that it will show up upon examining these ten systems. In Table I, we have given the average NN separation, $(a_M+a_N)/2$, using experimental values for the bulk metals. Upon examining how close these values lie to a_S=2.70 Å, one might expect (using the simple criterion mentioned above) that Fe-Au, Fe-Ag, Co-Au, and Co-Ag might be good candidates for forming strain-stabilized surface alloys, and Fe-Cd, Co-Cd, Fe-Pt, and Co-Pt may be possibilities, but Fe-Pb and Co-Pb surface alloys should be highly unlikely to form. As we will show below, these simple-minded expectations are not necessarily borne out.

Of the ten systems we consider in this paper, we are aware of previous studies on only two of them: Co-Ag/Ru(0001) (Refs. 12 and 13) and Fe-Ag/Ru(0001).[15] In both these cases, it was found that chemical interactions dominate over elastic ones, and the atomically mixed phase is disfavored.

II. COMPUTATIONAL DETAILS

Our calculations are done using *ab initio* spin-polarized density-functional theory with the PWscf package of the Quantum-ESPRESSO distribution.[16] However, in order to gauge the effects of magnetism, we have also performed some calculations in which spin polarization is suppressed. A plane-wave basis set is used with a kinetic-energy cutoff of 20 Ry. The charge-density cutoff value is taken to be 160 Ry. Ultrasoft pseudopotentials[17] are used to describe the interaction between ions and valence electrons. For the exchange-correlation functional, a generalized gradient approximation (GGA) of the Perdew-Burke-Ernzerhof form[18] is used. As all the systems are metallic, the Methfessel-Paxton smearing technique[19] is used with the smearing width equal to 0.05 Ry.

Convergence with respect to the basis size and the k-point grid has been carefully verified. For the bulk structure calculations, we have used the common crystal phase of each element. The k points used for Brillouin-zone integrations form an $8\times8\times8$ Monkhorst-Pack grid[20] for bulk calculations, and a $4\times4\times1$ grid for surface calculations. To study the surface properties, the supercell approach is used, with a unit cell that includes a slab and some vacuum layers. The slab used corresponds to a 2×2 surface unit cell, and contains six Ru layers to model the substrate. Our results for the energetics were obtained with one alloy overlayer (deposited on one side of the substrate) and seven vacuum layers (approximately 17.4 Å); we have allowed the alloy overlayer and the three topmost layers of Ru to relax, using Hellmann-Feynman forces. However, when performing calculations to see how the surface stress of monolayers of M or N on S varied with in-plane distance, the monolayer was deposited symmetrically on both sides of the slab, and the central layers of the slab were held fixed, while the outer layers on both sides were allowed to relax.

The (0001) surface of Ru is a closed-packed surface, on which typically one of the hollow sites, either hexagonal-closed packed (hcp) or face-centered cubic (fcc), is energetically preferred. We have allowed for both possibilities. The use of a (2×2) unit cell enables us to study five different compositions as shown in Fig. 1. Because of the small size of the unit cell, there is only one distinct configuration corresponding to each composition.

In this particular study, we have considered only a single pseudomorphic ordered layer of an alloy on the substrate slab. Our assumption that the monolayer (of either a single metal or an alloy) remains pseudomorphic was motivated by the general observation that reconstruction in the overlayer occurs only after a certain critical thickness of deposited material. For most systems studied previously consisting of a single metal on Ru(0001), it is found that the first overlayer of the metal does not reconstruct. However, Ag on Ru(0001) is an exception, in which a misfit dislocation structure has been observed, even for submonolayer films.[6]

III. RESULTS AND DISCUSSION

The substrate element, Ru, has the hcp structure in the bulk. Upon optimizing the geometry for bulk Ru, using the experimental c/a ratio of 1.584, we obtain a (which is also the NN distance a_S) as 2.74 Å, which is close to the experimental value of 2.70 Å.[21] For bulk Fe, Co, Pt, Au, Ag, Cd, and Pb we obtain NN distances $a\equiv a_{\mathrm{bulk}}^{\mathrm{calc}}$ of 2.47, 2.49, 2.83, 2.93, 2.95, 3.04, and 3.56 Å, respectively. Again, all these numbers match very well with the corresponding experimental values. The calculated magnetic moments for bulk Fe and Co are 2.36 and $1.71\mu_B$ per atom, respectively, which are comparable with the corresponding experimental values of 2.22 and $1.72\mu_B$ per atom.

For a single-component monolayer on Ru(0001), we find that both the magnetic elements prefer to occupy the hcp sites; occupying instead the fcc sites costs about 75 meV per

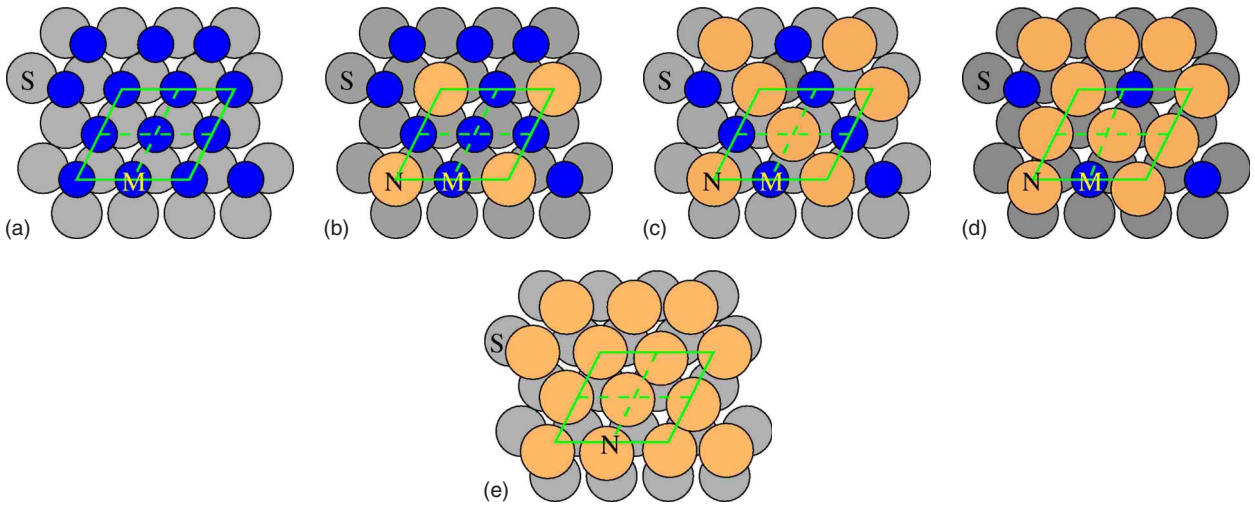

FIG. 1. (Color online) Top views of the systems studied, for x=(a) 1.00, (b) 0.75, (c) 0.50, (d) 0.25, and (e) 0.00. The rhombi (solid green lines) indicate the boundaries of the 2×2 surface unit cell. S denotes the substrate atoms (gray) and M and N denote magnetic (blue) and nonmagnetic (orange) elements, respectively.

surface atom. However, for all the nonmagnetic elements, with the exception of Pt, we find that the fcc site is very slightly favored over the hcp one, with an energy difference of the order of 4 meV per surface atom. In the rest of this paper, we work with the structures corresponding to the favored site occupancies for each system.

Upon depositing the single-component monolayers of either M or N on Ru(0001), and relaxing the geometry, we find that d_{12}, the interplanar distance between the overlayer and the topmost Ru layer, varies significantly depending upon the element constituting the overlayer. Our results for d_{12} are given in Table II; they may be compared with 2.17 Å, which is the value of $d_{\text{bulk}}^{\text{Ru}}$, the interplanar distance in bulk Ru. We see that for the M elements, $d_{12}<d_{\text{bulk}}^{\text{Ru}}$, whereas for the N elements, $d_{12}>d_{\text{bulk}}^{\text{Ru}}$. We also see a similar pattern upon examining our results for the surface stress of these systems (see Fig. 2): the M/Ru systems are under tensile stress, whereas all the N/Ru systems are under compressive stress. All these findings are consistent with the idea that the M atoms at the Ru surface would like to increase their ambient electron density, whereas the opposite is true for the N atoms; this is what one would expect from simple size considerations using the values of $a_{\text{bulk}}^{\text{calc}}$ for all the metals.

For the surface alloys, we find that in every case considered by us, the hcp site is favored over the fcc site. The difference in energy between the two sites varies from 10 to 70 meV per surface atom. Upon relaxing the alloy structures, we find that the surface layer can exhibit significant buckling; this follows the trends expected from the atomic-size mismatch between the constituent elements. Thus, Pt alloys do not show any visible buckling, while Pb alloys show the maximum amount of buckling among all the N's studied (see Fig. 3).

The total magnetic moment per magnetic atom, M_{tot}, is plotted in Fig. 4 as a function of fractional composition, x. Note that these moments include induced moments on the "nonmagnetic" overlayer atoms and the substrate atoms. In some cases, these induced moments are found to be appreciable. In most of the cases, the topmost layer of Ru atoms is spin polarized ferromagnetically with a magnetic moment ranging from 0.01 to $0.2\mu_B$ per atom. It is interesting to note that in all cases, with the single exception of Co-Pb/Ru, there is a significant enhancement in magnetic moments, with re-

TABLE II. Results for the value of d_{12}, the interplanar distance between the overlayer and topmost Ru layer, for single-component monolayers of M or N on the Ru(0001) substrate. It is interesting to compare these results with $d_{\text{bulk}}^{\text{Ru}}$=2.17 Å, which is the value of the interlayer distance in bulk Ru.

Elt.	Fe	Co	Pt	Au	Ag	Cd	Pb
d_{12} (Å)	2.08	2.01	2.30	2.49	2.45	2.51	2.55

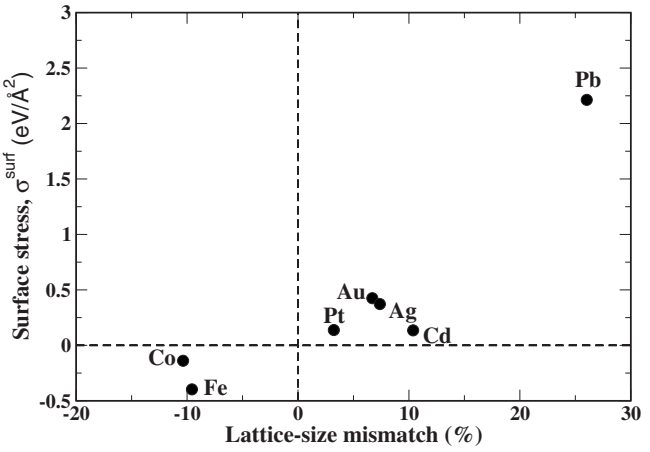

FIG. 2. Results for σ^{surf}, the diagonal component of the surface stress tensor, for a single-component monolayer of either M or N on Ru(0001), as a function of the lattice mismatch, defined as $(a-a_S)/(\frac{a+a_S}{2})$. Note that for the magnetic elements, $a<a_S$, and the surface stress is found to be tensile (negative), while for the nonmagnetic elements, $a>a_S$, and there is compressive (positive) surface stress.

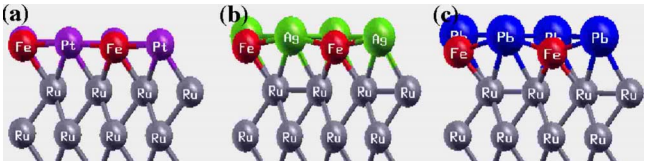

FIG. 3. (Color online) Relaxed geometries for surface alloys with $x=0.25$ for (a) Fe-Pt, (b) Fe-Ag, and (c) Fe-Pb. Here, gray, red, purple, green, and blue spheres represent Ru, Fe, Pt, Ag, and Pb atoms, respectively. Note that the amount of buckling increases progressively, in keeping with what one would expect upon considering the mismatch between the atomic sizes of the constituent elements.

spect to bulk Fe or Co. For Pt alloys, the enhancement in M_{tot} is most marked (because of significant moments induced on the Pt atoms); and there is a clear trend, where M_{tot} decreases monotonically as x in increased; this is in agreement with the Stoner argument. For all other cases, M_{tot} does not vary appreciably with x. In future work, we plan to analyze our results further to obtain a complete understanding of the magnetic behavior displayed by these systems.

The stability of an alloy phase relative to the phase-segregated phase can be determined by calculating the formation energy ΔH, which is defined as follows:

$$\Delta H = E_{\mathrm{slab}}(M_x N_{1-x}/S) - xE_{\mathrm{slab}}(M/S) - (1-x)E_{\mathrm{slab}}(N/S), \tag{1}$$

where $E_{\mathrm{slab}}(A/S)$ is the ground-state energy per surface atom for a single layer of A on the substrate S. When ΔH is negative, the two metals prefer to mix rather than to segregate, and hence the alloy phase is more stable.

Our results for ΔH as a function of composition from spin-polarized calculations are presented in Fig. 5 (solid lines). Note that in all cases, we find that ΔH is roughly

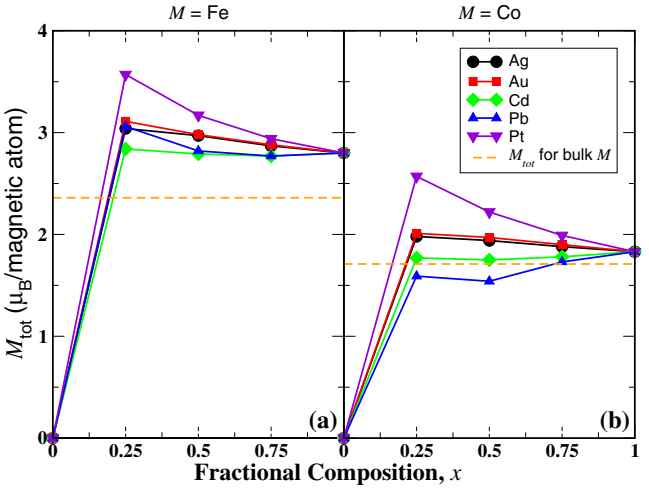

FIG. 4. (Color online) Results for how magnetic moments change upon alloying: the total magnetic moment per "magnetic atom" M is plotted as a function of the fractional composition x. The panels (a) and (b) contain results for Fe and Co alloys, respectively. For comparison, the magnetic moments of Fe and Co in their bulk structures are shown by dotted lines.

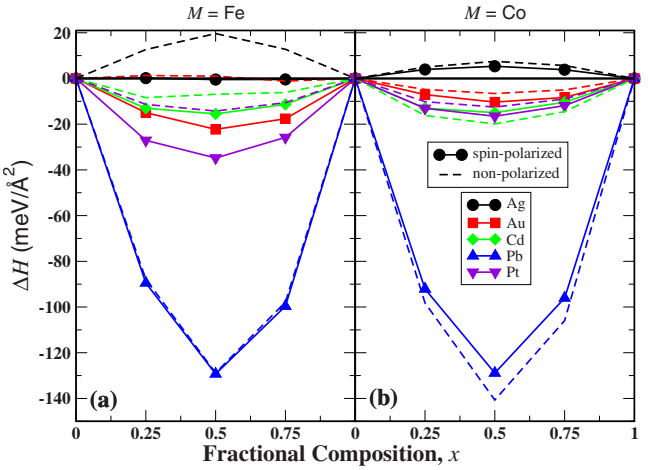

FIG. 5. (Color online) *Ab initio* results for ΔH, the formation energy per unit surface area: for each composition, the formation energy is plotted as a function of x, the fraction of the magnetic element M. The solid and dashed lines show the results obtained from spin-polarized and non-spin-polarized calculations, respectively. The panels on the left and right contain results for Fe and Co alloys, respectively. Note that Pb alloys are the most stable, followed by Pt, and Ag alloys are the least stable.

symmetric about $x=0.5$, suggesting that pairwise interactions are dominant. For both Fe and Co, alloys with Ag are found to be the least stable and alloys with Pb appear to be the most stable. However, though Fe and Co have almost the same $a_{\mathrm{bulk}}^{\mathrm{calc}}$, the values of ΔH, and even the order of stability, are not identical in the two cases. Similarly, despite having very close values of $a_{\mathrm{bulk}}^{\mathrm{calc}}$, Au and Ag display very different behavior: alloys of the former are stable, whereas Fe-Ag alloys are right at the boundary of stability, and Co-Ag alloys are unstable. These observations support the view that chemical effects may, in some cases, be quite important—and even dominate over elastic interactions. Our finding that atomic-level mixing is disfavored for Fe-Ag and Co-Ag is in keeping with the observations of previous authors.[12,13,15] We point out that our results underline the fact that $(a_M+a_N)/2 \approx a_S$ need not necessarily be a good criterion for atomic-level mixing to be favored (see Table I).

We analyze in detail the miscibility trends for ΔH obtained from spin-polarized calculations. It is generally accepted that there are two main contributions to the stability of such surface alloys: an elastic contribution and a chemical contribution.[13,22] We would like to separate out the two, if possible. In order to do so, we assume that the elastic interactions are given by a sum of NN contributions, with each pairwise term taking the form of a Morse potential,

$$V_{ij}(r) = A_0^{ij}\{1 - \exp[-A_1^{ij}(r - b^{ij})]\}^2, \tag{2}$$

where r is the distance between the NN atoms i and j, b^{ij} is the equilibrium bond length, and A_0^{ij} and A_1^{ij} are parameters related to the depth and width, respectively, of the potential well.

For each composition, the elastic energy is written as the sum of individual bond energies of the Morse form, by counting the total number of M-M, N-N, and M-N bonds in

each (2×2) unit cell. Accordingly, for $x=0.25$, 0.5, and 0.75, we obtain the elastic contribution to the formation energy as

$$\Delta H^{\rm ela}_{0.25} = 6V_{MN}(a_S) - 3V_{MM}(a_S) - 3V_{NN}(a_S), \quad (3)$$

$$\Delta H^{\rm ela}_{0.50} = 8V_{MN}(a_S) - 4V_{MM}(a_S) - 4V_{NN}(a_S), \quad (4)$$

$$\Delta H^{\rm ela}_{0.75} = 6V_{MN}(a_S) - 3V_{MM}(a_S) - 3V_{NN}(a_S). \quad (5)$$

Note that Eqs. (3) and (5) are identical, i.e., within our model, the elastic interactions lead to a $\Delta H^{\rm ela}$ that is symmetric about $x=0.5$. It is also important to note that for bulk alloys of M and N, there are no terms analogous to the second and third terms on the right-hand sides of the above equations. Due to the presence of the substrate, these terms have to be evaluated not at b^{MM} or b^{NN} (where they would lead to a zero contribution) but at the substrate spacing a_S. As a result of this, one can expect mixing rules to be quite different for surface alloys than for bulk alloys; we will return to this point further below.

In order to evaluate Eqs. (3)–(5), we need values for the Morse parameters A_0, A_1, and b, which appear in Eq. (2). We obtain these by computing the surface stress, $\sigma^{\rm surf}$, for each single-component monolayer as a function of the in-plane bond length l_{xy}. In principle, this could be obtained by compressing or expanding a monolayer of M or N on S. However, this would make the overlayer incommensurate with the substrate, leading to a surface unit cell which is too large for practical computation. Hence, we instead compress or expand the whole slab to perform calculations at different l_{xy}, and then subtract out the contribution from the substrate layers to the total stress so as to get the surface stress at each l_{xy}.[23] In order to carry out this procedure, we separate out the various contributions to the stress in the slab, as follows:

$$(\sigma^{V,\rm slab}_{xx})L_z = 2\sigma^{\rm surf}(l_{xy}) + (n_a-3)\sigma^{V,\rm bulk}_{xx}\frac{c}{2} + \frac{c}{2}\left[\sigma^{V,\rm bulk}_{xx} - \sigma^{V,\rm bulk}_{zz}\frac{2l^2_{xy}}{3c^2}\right]. \quad (6)$$

Here, $\sigma^{V,\rm slab}_{\alpha\alpha}$ is the $\alpha\alpha$ component of the "volume stress" for the slab (i.e., it has dimensions of force per unit area, as opposed to the surface stress, which has dimensions of force per unit length) for a slab with n_a atomic layers and length L_z (which includes the vacuum) along z, $\sigma^{\rm surf}(l_{xy})$ is the surface stress at an intraplanar bond length l_{xy}, and $\sigma^{V,\rm bulk}_{\alpha\alpha}$ is the $\alpha\alpha$ component of the volume stress for a bulk Ru cell that has been stretched or compressed in-plane to the same l_{xy} as the slab. In the equation above, the volume stresses have been multiplied by the corresponding lengths along the z direction so as to obtain quantities that have the same dimension as surface stress. Note that these geometrical factors are specific to the hcp structure; c is twice the interlayer distance along $z=[0001]$ direction for bulk Ru. The left-hand side of Eq. (6) consists of the stress for the slab with (n_a-2) substrate layers sandwiched between the two overlayers. As d_{12} is relaxed on both sides of the slab, within a nearest-neighbor approximation, this stress has contributions from (a) intralayer bonds in the two overlayers; this is the first term on the right-hand side of Eq. (6), (b) (n_a-2) sets of intralayer substrate bonds, and (c) (n_a-3) sets of interlayer substrate bonds. We can group these latter two terms as (i) (n_a-3) sets of interlayer +intralayer terms, and (ii) one additional set of intralayer terms. The first of these, i.e., the term corresponding to (i), is related simply to the xx component of the stress in a bulk Ru crystal; this is the second term on the right-hand side of Eq. (6). Finally, since interlayer terms but not intralayer terms contribute to $\sigma^{V,\rm bulk}_{zz}$, but both interlayer and intralayer terms contribute to $\sigma^{V,\rm bulk}_{xx}$, in order to obtain an expression for (ii), one can deduce the contribution to $\sigma^{V,\rm bulk}_{xx}$ from intralayer terms alone, by comparing appropriately scaled values of $\sigma^{V,\rm bulk}_{xx}$ and $\sigma^{V,\rm bulk}_{zz}$; this is the last term in Eq. (6). Thus the surface stress is now given by the expression

$$\sigma^{\rm surf}(l_{xy}) = \frac{1}{2}\left[(\sigma^{V,\rm slab}_{xx})L_z - (n_a-2)\sigma^{V,\rm bulk}_{xx}\frac{c}{2} + \sigma^{V,\rm bulk}_{zz}\frac{l^2_{xy}}{3c}\right]. \quad (7)$$

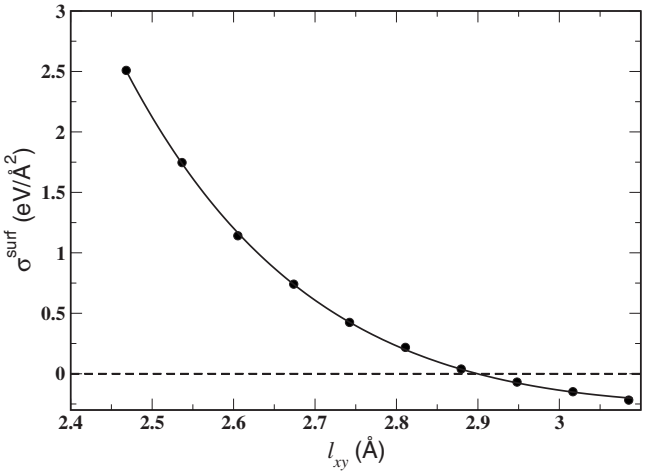

FIG. 6. $\sigma^{\rm surf}$ versus l_{xy} for Au/Ru(0001): The value of $\sigma^{\rm surf}$ at each l_{xy} is computed by compressing or stretching the complete slab, and then subtracting out the contribution of substrate layers. The data points are fitted by an expression derived from a Morse potential, to get the values of A_0, A_1, and b for Au-Au bonds. The dots represent *ab initio* results, while the solid curve is the Morse fit.

The Morse parameters for an i-i bond can be extracted from the plot of $\sigma^{\rm surf}$ versus l_{xy} for each single-component overlayer of M or N on the Ru surface. As an example, our results for the variation in surface stress with in-plane strain, for a monolayer of Au on Ru(0001), are shown in Fig. 6; qualitatively similar curves are obtained for other elements. The value of b^{MM} or b^{NN} is given by the value of l_{xy} at which the graph crosses the x axis, while the values of A_0 and A_1 are obtained by fitting the curve to an expression derived from a Morse potential. The values thus obtained for all seven overlayer elements are given in Table III. The value of b^{ii} serves as a measure of the effective size of an atom i when placed on the Ru(0001) surface. Note that for both the magnetic elements M, b^{MM} is smaller than a_S, whereas for all the nonmagnetic elements N considered by us, b^{NN} is greater than a_S. However, the values of b are found to be different

TABLE III. Values for the Morse parameters for M-M and N-N interactions, as deduced from surface stress calculations. The last column contains our values for the calculated nearest-neighbor spacing for M or N in their bulk structures. These may be compared with our values for b, which is the preferred interatomic spacing for a monolayer of M or N on Ru(0001).

M/N	A_0 (eV)	A_1 (Å^{-1})	b (Å)	$a_{\text{bulk}}^{\text{calc}}$ (Å)
Fe	0.1309	2.412	2.56	2.47
Co	0.5827	2.052	2.37	2.49
Pt	0.6744	1.817	2.79	2.83
Au	0.4341	1.797	2.90	2.93
Ag	0.3638	1.669	2.92	2.95
Cd	0.6564	1.680	2.79	3.04
Pb	0.2027	1.563	3.42	3.56

from $a_{\text{bulk}}^{\text{calc}}$, in some cases quite significantly so. This difference is due to the presence of both the surface (i.e., no neighbors above) and the substrate (different neighbors below). It is interesting to note that for Fe/Ru(0001), $b > a_{\text{bulk}}^{\text{calc}}$, whereas for all the other elements, $b < a_{\text{bulk}}^{\text{calc}}$. This is presumably because Fe in the bulk form has the body-centered cubic (bcc) structure with a coordination number of 8, whereas all the other elements have either the fcc or hcp structure with 12-fold coordination. As a result, only for Fe are the overlayer atoms more effectively coordinated when placed on a Ru surface. However, apart from such general observations, we were unable to discern any simple relationship connecting the values of b and $a_{\text{bulk}}^{\text{calc}}$.

It remains to obtain the Morse parameters for M-N bonds. In analogy with the Lorentz-Berthelot mixing rules, the M-N bond parameters are assumed to have the form $b^{MN}=(b^{MM}+b^{NN})/2$, $A_0^{MN}=\sqrt{A_0^{MM}A_0^{NN}}$, and $A_1^{MN}=\sqrt{A_1^{MM}A_1^{NN}}$. An examination of our results for the surface stress σ^{surf} of the mixed alloy phases suggests that these approximations do not introduce large errors. For example, we consider the cases of alloys of Fe with Pt (the smallest N) and Pb (the largest N): we compare our values of σ^{surf} for $Fe_{0.25}Pt_{0.75}/Ru$ and $Fe_{0.25}Pb_{0.75}/Ru$ obtained from *ab initio* results (0.028 and 1.211 eV/Å^2, respectively) with those obtained using the Lorentz-Berthelot mixing rules (0.026 and 1.312 eV/Å^2, respectively); the values from the two approaches match well. We believe that while some of the (slight) discrepancy is due to the use of the mixing rules, some may also be due to our assumption that the interatomic interactions have the form of a Morse potential. In Table IV we have tabulated the values of b^{MN}. These should be compared to the bulk Ru NN spacing (=2.74 Å). It is also instructive to compare the values in Table IV with those in Table I; one finds that there is no dramatic change upon accounting for altered surface sizes.

TABLE IV. Values of b^{MN}, obtained by taking the average of preferred nearest-neighbor spacing on the surface; these values should be compared to our calculated value of 2.74 Å for the NN distance on the Ru substrate.

b^{MN} (Å)	Pt	Au	Ag	Cd	Pb
Fe	2.67	2.73	2.74	2.67	2.99
Co	2.58	2.63	2.64	2.58	2.89

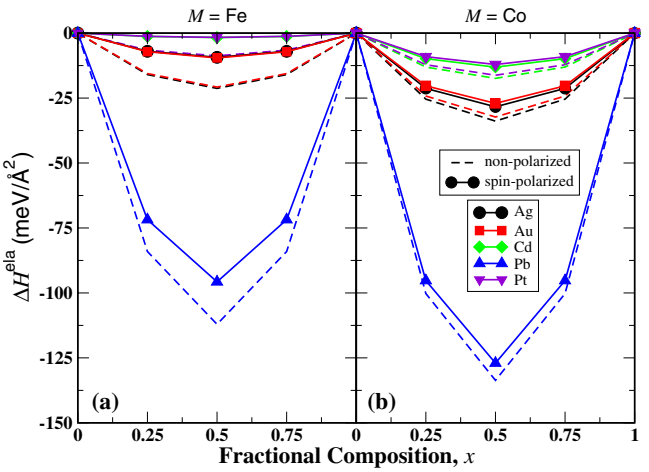

FIG. 7. (Color online) Results for the elastic contribution to the formation energy: ΔH^{ela} is plotted as a function of fractional composition x, for (a) Fe and (b) Co alloys, for both spin-polarized (solid lines) and non-spin-polarized calculations (dashed lines). Note that, from elastic considerations, spin polarization always makes mixing less favorable.

Our results for the elastic contribution to the formation energy, evaluated using Eqs. (3)–(5), are displayed in Fig. 7 (solid lines). We find that for all ten combinations considered by us, elastic interactions always favor mixing of the two overlayer elements, in accordance with the predictions by Tersoff.[5]

At first sight, our most surprising result appears to be our finding that for both magnetic elements, the Pb alloys are the most stable, though upon examining Table I or Table IV, one might think that this is unlikely. However, this is because for surface alloys, unlike bulk alloys, the phase-segregated forms can cost a high elastic energy because of the presence of the substrate. Since pseudomorphic Pb/Ru(0001) costs a great deal in elastic energy, the mixed form is correspondingly favored. In order to make this argument clearer, in Fig. 8, we have separated out the individual contributions to the right-hand side of Eq. (4). The first (M-N) term is always positive, while the second (M-M) and third (N-N) terms are always negative. In order for ΔH to be negative, the first term should be small (the simple mixing rule applies only to this term), while the second and third terms should be large in magnitude. The first term is found to follow the expectations from an elementary consideration of sizes (either at the bulk or at the surface): Ag and Au alloys are the most favored, followed by Pt and Cd, and then Pb. It is interesting to note that both Cd and Pt alloys have roughly the same contribution from this first term; this is because Cd undergoes a relatively large contraction in size at the surface, relative to the bulk. A Co monolayer on Ru(0001) is relatively unhappy (i.e., the contribution to the elastic part of the formation energy is significant and negative), and a Pb monolayer on Ru(0001) is extremely unfavorable energetically. As a result of these two facts, elastic interactions favor the formation of Co-N alloys over Fe-N alloys, and lead to the high stability

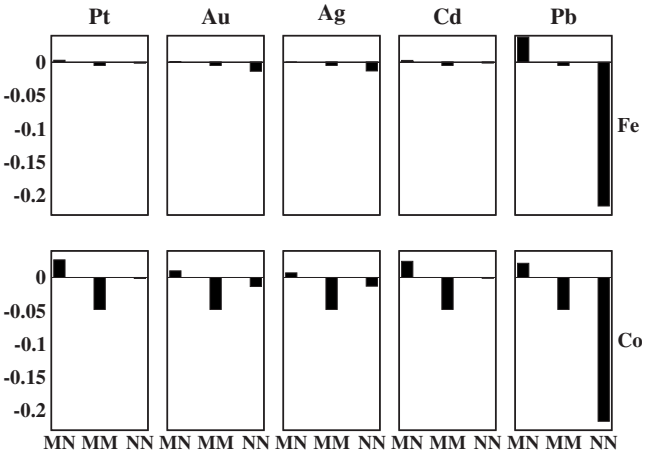

FIG. 8. The various contributions [from Eq. (4)] to ΔH^{ela} in units of meV/Å^2, for $x=0.5$, for the spin polarized case. The upper panel is for Fe-N and the lower panel is for Co-N alloys. Contributions from M-N, M-M, and N-N bonds are displayed separately. All the histograms have been plotted on the same scale, to make comparison easier. Note the very high negative contribution from Pb-Pb bonds for both Fe-Pb and Co-Pb alloys.

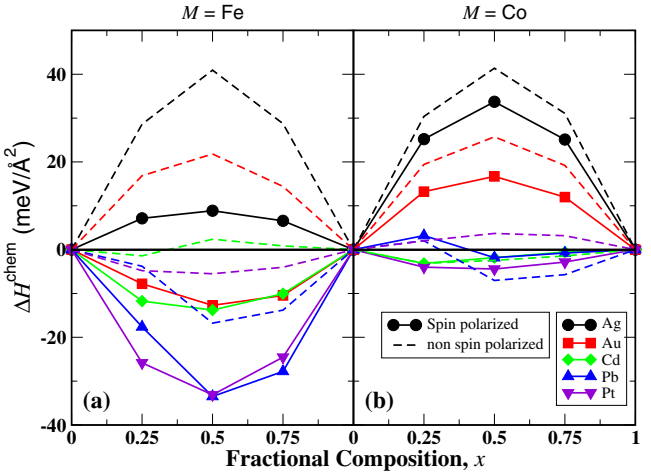

FIG. 9. (Color online) The chemical contribution to the alloy formation energy, as a function of fractional composition x, for (a) Fe and (b) Co surface alloys on Ru(0001). The solid lines show the results from spin-polarized calculations and the dashed lines are for non-spin-polarized calculations.

against phase segregation of M-Pb alloys. However, one should be cautious in interpreting these results since we have made the assumption that the alloys as well as phase-segregated monolayers remain pseudomorphic. For the alloys, this is probably a valid assumption since the elastic energy is small, i.e., the stress is unlikely to be high enough to drive the overlayer to relax. Despite the significant elastic energy contained in a Co/Ru(0001) monolayer, it does not reconstruct.[24] However, for Pb/Ru(0001), the very high elastic energy makes it seem possible that this system might reconstruct, presumably via a network of misfit dislocations; we are not aware of any experimental information on this system. Thus, the high stability we obtain for M-Pb alloys may be misleading; the stability would be lowered if the phase-segregated form were to reconstruct (since the third term in the elastic energy would then be decreased in magnitude).

Finally, in Fig. 9 (solid lines), we display our results for the chemical contribution to the formation energy ΔH^{chem}, obtained by subtracting out the data in Fig. 7 from that in Fig. 5. When only chemical interactions are considered, Fe alloys are more favorable than Co alloys; we will show further below that this can be attributed to the larger magnetic moment of Fe. From this plot, we note that the stability of Pt alloys is largely due to the favored chemical bonds between Fe-Pt and Co-Pt ; this is consistent with the fact that these systems also form bulk alloys. The Ag alloys are not stable because Co-Ag and Fe-Ag bonds cost very high chemical energy, which cannot be offset by elastic energy; this too is consistent with previous results.[12,13,15] Also note that Fe-Au bonds favor mixing, whereas Co-Au bonds cost chemical energy, which explains the particular order of stability observed in the *ab initio* results.

How does magnetism affect miscibility? Previous studies have shown that magnetism can affect mixing in surface alloys.[25] To examine this issue, we have also performed non-spin-polarized (NSP) total-energy calculations on these systems. The dashed lines in Fig. 5 show the NSP results for ΔH as a function of x. For all the systems, except for Co-Cd and Co-Pb, mixing is more favorable when the systems are spin polarized (SP) than when magnetism is suppressed, which is in accordance with earlier observations.[25] As a result, Fe-Ag alloys, which are at the boundary of miscibility when spin polarized, are immiscible in the absence of magnetism. The difference between SP and NSP results is more pronounced for Fe alloys than for Co alloys (with the single exception of Fe-Pb), which can be attributed to the higher magnetic moments on the Fe-N/Ru(0001) systems. It is interesting to note that the two systems (Co-Cd and Co-Pb) for which the miscibility is increased upon suppressing the spin polarization are also the only two systems for which M_{tot} per magnetic atom is less for the alloy phases than for M/Ru.

We now repeat our computation of elastic and chemical contributions to ΔH, for the NSP case. As expected, for Fe and Co, the NSP values of b—the effective size on the surface (=2.45 and 2.36 Å, respectively)—are less than the SP ones (see Table III). The percentage decrease is more for Fe (~4%) as compared to Co (~0.4%), which can be attributed to the higher magnetic moment of the Fe monolayer. The computed elastic contribution to the NSP ΔH is plotted in Fig. 7 (dashed lines). It shows that when elastic effects alone are considered, spin polarization disfavors mixing. On examining the separate contributions to ΔH^{ela} from M-M, N-N, and M-N bonds, we find that the main reason for the reduced miscibility of SP phases is that the M monolayer is relatively less stressed when spin polarized. The difference between the SP and NSP values of ΔH is more for Fe alloys than for Co alloys, as a direct consequence of the larger decrease in b for Fe.

The chemical contribution to the heat of formation, ΔH^{chem}, for NSP alloys is plotted in Fig. 9 (dashed lines). It is interesting to note that in the absence of magnetism the chemical interactions for Fe and Co are rather similar. This

implies that the presence of magnetic moments alters the chemical interactions to a great extent. In general, when considering the chemical contribution terms, spin polarization promotes mixing in all the cases, except for Co-Cd and Co-Pb. For chemical interactions also, the difference between the SP and NSP values of ΔH is more for Fe alloys than for Co alloys because of the larger magnetic moment on Fe alloys.

From our analysis, it appears that while considering the effects on miscibility as one switches on spin polarization, chemical interactions generally drive the system toward mixing ($\Delta H_{\mathrm{SP}}^{\mathrm{chem}} < \Delta H_{\mathrm{NSP}}^{\mathrm{chem}}$), while elastic interactions do the opposite ($\Delta H_{\mathrm{SP}}^{\mathrm{ela}} > \Delta H_{\mathrm{NSP}}^{\mathrm{ela}}$). The changes in the chemical interactions are more in magnitude, and hence the systems are more miscible when magnetized, except for the two combinations (Co-Cd and Co-Pb) where both elastic and chemical interactions raise ΔH upon switching on spin polarization.

IV. SUMMARY AND CONCLUSIONS

In this paper, we have attempted to gain an understanding of the factors governing the energetics of strain-stabilized surface alloys, by performing *ab initio* calculations on ten combinations involving a magnetic and a nonmagnetic metal co-deposited on a Ru(0001) substrate. In many cases, we find the surface alloy to be stable against phase segregation, even though the constituent elements are immiscible in the bulk.

We have also studied some of the magnetic properties and observe enhanced magnetic moments for the surface alloys as compared to bulk magnetic moments. The effects of magnetism on the miscibility of these alloys have also been studied. In general, we observe that magnetism promotes mixing.

We find that the results for miscibility do not correlate with expectations based upon the simple argument that the mean atomic size should be as close as possible to the substrate lattice spacing. One reason for this is that though elastic interactions are an important mechanism governing stability, chemical interactions can also play a crucial role. In some cases, the latter are large enough to disfavor atomic-level mixing, even if it helps in lowering the elastic energy. A second complicating factor is that unlike for bulk alloys, for such strain-stabilized surface alloys, the phase-segregated forms can also cost elastic energy. Thus, there are three factors that determine whether or not mixing takes place at the atomic level: (i) the elastic energy of the alloy phase, (ii) the elastic energies of the phase-segregated monolayers on the substrate, and (iii) chemical interactions. Further, all three of these factors can be affected by the presence of magnetism. Because of this complicated situation, a simple criterion, analogous to the first Hume-Rothery rule for bulk alloys, does not seem possible for such systems.

We have also found that effective atomic sizes on the Ru substrate are not equal to the bulk size; in some cases this difference is small, while in other cases it is large. Several alloys involving a magnetic and a nonmagnetic element on a Ru(0001) surface are found to be stable against phase segregation; this is primarily because the effective size of the magnetic elements is smaller than the nearest-neighbor distance in the substrate, while that of the nonmagnetic elements is larger, even after accounting for altered sizes at the surface. Of the systems we have considered, we feel that Fe-Au, Fe-Cd, and Co-Cd are particularly promising candidates that would be worth experimental investigation. In these systems, both chemical and elastic interactions promote alloying. We have also found that surface alloys involving Pb and either Fe or Co appear to be very resistant to phase segregation; however, this conclusion is dependent on our assumption that a monolayer of Pb on Ru(0001) does not reconstruct, which may or may not be valid.

ACKNOWLEDGMENTS

We acknowledge helpful discussions with Sylvie Rousset, Vincent Repain, and Yann Girard. Funding was provided by the Indo-French Centre for the Promotion of Advanced Research. Computational facilities were provided by the Centre for Computational Material Science at JNCASR.

[1] W. Hume-Rothery, R. E. Smallman, and C. W. Hayworth, *The Structure of Metal and Alloys* (The Metals and Metallurgy Trust, London, 1969).
[2] L. Pleth Nielsen, F. Besenbacher, I. Stensgaard, E. Lægsgaard, C. Engdahl, P. Stoltze, K. W. Jacobsen, and J. K. Nørskov, Phys. Rev. Lett. **71**, 754 (1993).
[3] H. Röder, R. Schuster, H. Brune, and K. Kern, Phys. Rev. Lett. **71**, 2086 (1993).
[4] J. Neugebauer and M. Scheffler, Phys. Rev. Lett. **71**, 577 (1993).
[5] J. Tersoff, Phys. Rev. Lett. **74**, 434 (1995).
[6] R. Q. Hwang, J. C. Hamilton, J. L. Stevens, and S. M. Foiles, Phys. Rev. Lett. **75**, 4242 (1995).
[7] J. L. Stevens and R. Q. Hwang, Phys. Rev. Lett. **74**, 2078 (1995).
[8] M. Schick, J. Schäfer, K. Kalki, G. Ceballos, P. Reinhardt, H. Hoffschulz, and K. Wandelt, Surf. Sci. **287-288**, 960 (1993).
[9] M. Schick, G. Ceballos, Th. Peizer, J. Schäffer, G. Rangelov, J. Stober, and K. Wandelt, J. Vac. Sci. Technol. A **12**, 1795 (1994).
[10] B. Sadigh, M. Asta, V. Ozoliņš, A. K. Schmid, N. C. Bartelt, A. A. Quong, and R. Q. Hwang, Phys. Rev. Lett. **83**, 1379 (1999).
[11] J. Yuhara, M. Schmid, and P. Varga, Phys. Rev. B **67**, 195407 (2003).
[12] G. E. Thayer, V. Ozolins, A. K. Schmid, N. C. Bartelt, M. Asta, J. J. Hoyt, S. Chiang, and R. Q. Hwang, Phys. Rev. Lett. **86**, 660 (2001).
[13] G. E. Thayer, N. C. Bartelt, V. Ozolins, A. K. Schmid, S. Chiang, and R. Q. Hwang, Phys. Rev. Lett. **89**, 036101 (2002).
[14] E. D. Tober, R. C. F. Farrow, R. F. Marks, G. Witte, K. Kalki, and D. D. Chambliss, Phys. Rev. Lett. **81**, 1897 (1998).
[15] B. Yang, T. Muppidi, V. Ozolins, and M. Asta, Phys. Rev. B **77**, 205408 (2008).
[16] S. Baroni, S. de Gironcoli, A. Dal Corso, and Paolo Giannozzi, http://www.pwscf.org/
[17] D. Vanderbilt, Phys. Rev. B **41**, 7892 (1990).

[18] J. P. Perdew, K. Burke, and M. Ernzerhof, Phys. Rev. Lett. **77**, 3865 (1996).
[19] M. Methfessel and A. T. Paxton, Phys. Rev. B **40**, 3616 (1989).
[20] H. J. Monkhorst and J. D. Pack, Phys. Rev. B **13**, 5188 (1976).
[21] N. W. Ashcroft and N. D. Mermin, *Solid State Physics* (Thomson Asia Pte. Ltd., Bangalore, 2004).
[22] V. Ozoliņš, M. Asta, and J. J. Hoyt, Phys. Rev. Lett. **88**, 096101 (2002).
[23] R. Pushpa and S. Narasimhan, Phys. Rev. B **67**, 205418 (2003).
[24] R. Q. Hwang, C. Günther, J. Schröder, S. Günther, E. Kopatzki, and R. J. Behm, J. Vac. Sci. Technol. A **10**, 1970 (1992).
[25] S. Blügel, Appl. Phys. A: Mater. Sci. Process. **63**, 595 (1996).